

CO Oxidation Promoted by the Gold Dimer in Au_2VO_3^- and Au_2VO_4^- Clusters

Li-Na Wang, Zi-Yu Li, Qing-Yu Liu, Jing-Heng Meng, Sheng-Gui He,* and Tong-Mei Ma*

Abstract: Investigations on the reactivity of atomic clusters have led to the identification of the elementary steps involved in catalytic CO oxidation, a prototypical reaction in heterogeneous catalysis. The atomic oxygen species O^- and O_2^{2-} bonded to early-transition-metal oxide clusters have been shown to oxidize CO. This study reports that when an Au_2 dimer is incorporated within the cluster, the molecular oxygen species O_2^{2-} bonded to vanadium can be activated to oxidize CO under thermal collision conditions. The gold dimer was doped into Au_2VO_4^- cluster ions which then reacted with CO in an ion-trap reactor to produce Au_2VO_3^- and then Au_2VO_2^- . The dynamic nature of gold in terms of electron storage and release promotes CO oxidation and O–O bond reduction. The oxidation of CO by atomic clusters in this study parallels similar behavior reported for the oxidation of CO by supported gold catalysts.

Oxide-supported gold catalysts have attracted significant interest after the discovery of their extraordinary activity for catalytic CO oxidation at low temperature.^[1–4] The mechanistic details proposed in several reports regarding the nature of active sites, the catalytic role of gold, as well as the oxide supports are often controversial.^[5,6] An important topic in the mechanistic study is the activation of molecular oxygen and the catalytically active oxygen species that are present under the working conditions of gold catalysis.^[3,4,7] Superoxide radicals ($\text{O}_2^{\cdot-}$), peroxides (O_2^{2-}), atomic oxygen radicals (O^-), and lattice oxygen (O^{2-}) are four typical oxygen species (OS) involved in the O_2 activation and dissociation processes: $\text{O}_2 \rightarrow \text{O}_2^{\cdot-} \rightarrow \text{O}_2^{2-} \rightarrow 2\text{O}^- \rightarrow 2\text{O}^{2-}$.^[8] It has been proposed that the OS are usually supplied by the oxide supports in gold catalysis.^[3,4,9,10] The reactions of CO with various OS can be characterized by Raman, infrared, and electron spin resonance spectroscopic methods in condensed-phase studies. However, these techniques would not be suitable to follow the elementary reactions proposed in Equations (1)–(4).



Gas-phase studies of CO oxidation by atomic clusters under well controlled and reproducible conditions using state-of-the-art mass spectrometry (MS) and quantum chemistry calculations provide an alternative approach to understanding the elementary reactions (1)–(4) at the molecular level (ML).^[11] To investigate the ML mechanism of CO oxidation on oxide-supported gold (Au/MO_x), it is important to study not only the gold clusters (Au_x)^[11,12] and the homonuclear oxide clusters (M_xO_y ; where, for example, $\text{M} = \text{Ti}, \text{V}$)^[11,13] but also the gold-containing heteronuclear oxide clusters ($\text{Au}_x\text{M}_y\text{O}_z$).^[14] Cluster studies have identified that reaction (3) can take place on many early-transition-metal (ETM) oxide clusters, such as $(\text{TiO}_2)_n\text{O}^-$, $(\text{ZrO}_2)_n^+$, and $\text{V}_4\text{O}_{10}^+$, under thermal collision conditions.^[13] So far, no convincing evidence for reactions (1), (2), and (4) on homonuclear ETM oxide clusters has been reported.^[11,13] By studying ETM clusters $\text{AuTi}_x\text{O}_y^-$ doped with a single Au atom we have recently identified that reaction (4) is promoted by the gold monomer.^[14a] This study reports that the cluster Au_2VO_4^- , doped with a gold dimer, can activate the peroxide species O_2^{2-} bonded to the ETM to oxidize CO molecules [Eq. (2)] under thermal collision conditions.

The $\text{Au}_2\text{V}^{18}\text{O}_x^-$ cluster ions ($x = 3$ and 4) were generated by laser ablation, mass-selected, thermalized, and then reacted with C^{16}O in an ion-trap reactor.^[15] The interactions of Au_2VO_4^- with N_2 generate the weak collision-induced dissociation (CID) product VO_4^- (Figure 1a1), suggesting that an Au_2 unit is only weakly bonded in the cluster. Upon the interaction of Au_2VO_4^- with CO, products Au_2VO_3^- and Au_2VO_2^- were produced (Figure 1a2). Most of the Au_2VO_3^- product ions could convert into Au_2VO_2^- at high CO pressure (Figure 1a3). Using the compound Au_2VO_3^- as the cluster source in reaction with CO, Au_2VO_2^- was formed (Figures 1b2 and 1b3). The products Au_2VO_3^- in Figure 1a2 and Au_2VO_2^- in Figure 1b2 were not generated in the cluster interactions with N_2 (Figures 1a1 and 1b1), which indicates that these products are due to the chemical reactions shown in Equations (5) and (6) rather than the CID processes:



[*] L.-N. Wang, Z.-Y. Li, Q.-Y. Liu, J.-H. Meng, Prof. S.-G. He
Beijing National Laboratory for Molecular Science
State Key Laboratory for Structural Chemistry of Unstable and Stable Species, Institute of Chemistry
Chinese Academy of Sciences, Beijing 100190 (China)
E-mail: shengguihe@iccas.ac.cn

L.-N. Wang, Prof. T.-M. Ma
School of Chemistry and Chemical Engineering
South China University of Technology
381 Wushan Road, Tianhe District, Guangzhou 510640 (China)
E-mail: tongmei@scut.edu.cn



Supporting information for this article is available on the WWW under <http://dx.doi.org/10.1002/anie.201505476>.

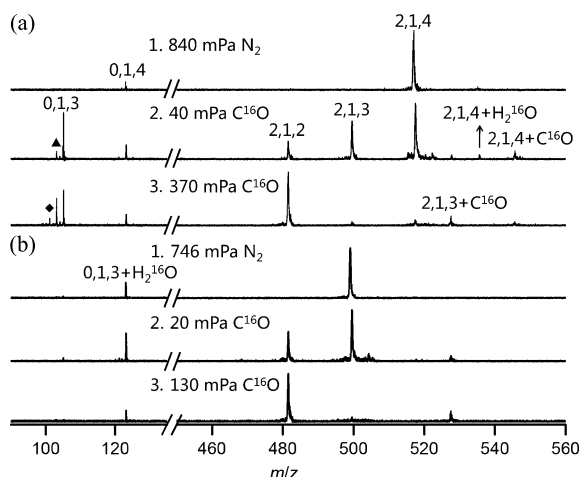


Figure 1. Time-of-flight mass spectra for the reactions of mass-selected a) $\text{Au}_2\text{V}^{18}\text{O}_4^-$ and b) $\text{Au}_2\text{V}^{18}\text{O}_3^-$ with gases C^{16}O (a2, a3, b2, and b3) and N_2 (a1 and b1) under different reactant gas pressures. The numbers above the mass spectral signals denote the numbers of atoms of Au, V, and O (x,y,z) in the compounds $\text{Au}_x\text{V}_y^{18}\text{O}_z^-$. The reaction time is 0.94 ms. Two signals marked with \blacktriangle and \blacklozenge can be assigned to $\text{V}^{18}\text{O}_2^{16}\text{O}^-$ and $\text{V}^{18}\text{O}^{16}\text{O}_2^-$, respectively.

In addition to the Au_2VO_3^- and Au_2VO_2^- products, the VO_3^- cluster was also generated from the reaction of Au_2VO_4^- with CO (Figures 1a2 and 1a3). $^{18}\text{O}/^{16}\text{O}$ exchange between $\text{V}^{18}\text{O}_3^-$ and C^{16}O as well as other minor reaction channels are described in the Supporting Information.

The pseudo-first-order rate constants (k_1) for the reactions of Au_2VO_4^- and Au_2VO_3^- with CO were estimated on the basis of a least-square fitting procedure (Figures S7 and S8).^[14c] Reactions (5) and (6) have rate constants of $(9 \pm 3) \times 10^{-11}$ and $(10 \pm 3) \times 10^{-11} \text{ cm}^3 \text{ molecule}^{-1} \text{ s}^{-1}$, which correspond to reaction efficiencies ($\varphi = k_1/k_{\text{ADO}}$, in which k_{ADO} is the collision rate constant computed on the basis of the average dipole orientation theory)^[16] of $(13 \pm 4)\%$ and $(14 \pm 4)\%$, respectively. The Au_2VO_3^- cluster may be slightly more reactive than Au_2VO_4^- .

Density functional theory (DFT) calculations indicated that the lowest-lying isomer of Au_2VO_4^- (Figure 2a and Figure S11) is a closed-shell species with one gold dimer, two O^{2-} ions, and a peroxide unit (O_2^{2-}). The Au_2 dimer is bonded to an O^{2-} ion in the cluster. The negatively charged gold atom (Au1 with a charge of -0.364 e) in Au_2VO_4^- can capture CO with a binding energy of 0.84 eV (Figure 2a, intermediate I1). The Au_2 dimer can deliver CO for oxidation by O^{2-} ($\text{I1} \rightarrow \text{I2} \rightarrow \text{I3}$) or by O_2^{2-} ($\text{I1} \rightarrow \text{I2} \rightarrow \text{I3}'$). Oxidation by O^{2-} ($\text{TS2} = -0.14 \text{ eV}$) is slightly more favorable than oxidation by O_2^{2-} ($\text{TS2}' = -0.06 \text{ eV}$). Reaction intermediate I3 rearranges into I4 with a small barrier (0.19 eV) and then the O_2^{2-} unit cleaves into two separate O^{2-} ions ($\text{I4} \rightarrow \text{I5}$). The CO_2 can be easily lost from I5 or I3'. The experimental observation of reaction (5) in Figure 1a2 is thus well supported by the DFT calculations, with the reaction calculated to be highly exothermic ($\Delta H_0 = -2.60 \text{ eV}$, Figure 2a) and all of the transition states (TSs) lower in energy than the separate reactants ($\text{Au}_2\text{VO}_4^- + \text{CO}$). It is noteworthy that the Au_2VO_3^- cluster formed in reaction (5) can have enough energy

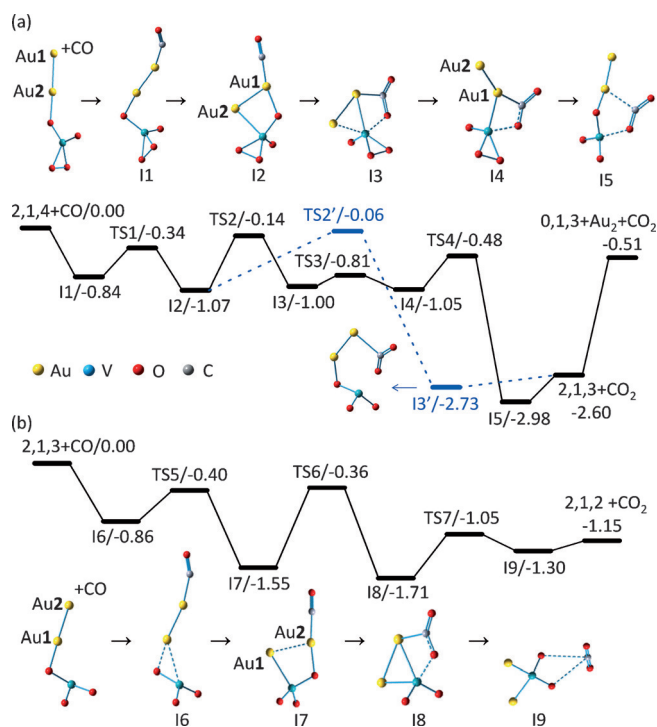


Figure 2. DFT-calculated potential energy profile for CO oxidation by a) Au_2VO_4^- and b) Au_2VO_3^- . The numbers given are the zero-point vibration corrected energies (eV) of the reaction intermediates (I1–I9), transition states (TS1–TS7), and products, with respect to the separated reactants. The structures of TS1–TS7 can be found in the Supporting Information. Product nomenclature: $\text{Au}_2\text{V}_i\text{O}_j^-$ (denoted 2,1, i); $\text{Au}_2\text{V}_i\text{O}_j^-$ (2,1, j); V_iO_j^- (0,1, j); and $\text{Au}_2\text{V}_i\text{O}_j^-$ (2,1,2).

(2.60 eV) to dissociate Au_2 from VO_3^- ($\text{Au}_2\text{VO}_3^- \rightarrow \text{VO}_3^- + \text{Au}_2$, $\Delta H_0 = 2.09 \text{ eV}$). This result explains the generation of VO_3^- in Figure 1a2.

The mechanism of CO oxidation by Au_2VO_3^- (Figure 2b) is similar to that by Au_2VO_4^- . Although the oxidation of CO by Au_2VO_3^- is less exothermic than by Au_2VO_4^- ($\Delta H_0 = -1.15 \text{ eV}$ versus -2.60 eV), the former is kinetically more favorable as can be seen from the critical TS energies ($\Delta H_0(\text{TS6}) = -0.36 \text{ eV}$ versus $\Delta H_0(\text{TS2}) = -0.14 \text{ eV}$). This calculation is consistent with the experimental result that reaction (6) is faster than reaction (5). As in Au_2VO_4^- , the gold dimer in Au_2VO_3^- is bonded to one O atom, while the Au–Au bond is cleaved and two Au–V bonds are formed during the late stage ($\text{I8} \rightarrow \text{I9}$) of reaction (6).

The oxidation of CO by atomic clusters has been extensively studied^[11–14] and the investigations on the oxide clusters of ETMs as well as main-group metals all emphasized the importance of the O^- radicals (reaction (3)). For example, the clusters containing O^- , specifically $(\text{MO}_2)_n\text{O}^-$ ($\text{M} = \text{Ti}, \text{Zr}, \text{Ce}$),^[13e,17] VO_3 ,^[13c] YAlO_3 ,^[18] VAlO_4 ,^[19] and many others,^[11] can react with CO through the O^- radical centers. In contrast, their oxygen-rich counterparts containing O_2^- , O^{2-} , and possibly O_2^{2-} species did not undergo reaction with CO in the reported experiments. Recent MS and DFT studies have identified that when the clusters had single Au atoms, CO oxidation by O^{2-} (reaction (4)) on closed-shell clusters

such as $\text{AuTi}_3\text{O}_{7.8}^-$ can be driven by conversion of the Au–O bonds into gold–metal bonds (such as Au–Ti).^[14a] It is noteworthy that in our experiments several vanadium oxide cluster anions doped with a single gold atom, such as AuVO_3^- and $\text{AuV}_3\text{O}_{8.9}^-$ (Figures S3–S5), could also react with CO to generate products in which one oxygen atom has been lost, although this study focused on the gold dimer system. The DFT study indicated that the conversion of one Au₂–O bond into two Au–V bonds could also drive the oxidation of CO by O^{2-} in the closed-shell species Au_2VO_3^- (Figure 2b). However, VO_3^- and VO_4^- clusters without gold do not oxidize CO (see the Supporting Information for more discussion).

The presence of a single gold atom (within the cluster) can promote the oxidation of CO by atomic OS on ETM oxide clusters. This result contrasts with previous cluster studies which indicated that it is difficult to activate molecular OS such as O_2^{2-} towards CO oxidation. For example, the O_2^{2-} unit in the $\text{AuTi}_3\text{O}_8^-$ cluster remains in the product cluster upon the oxidation of the first CO molecule ($\text{AuTi}_3\text{O}_8^- + \text{CO} \rightarrow \text{AuTi}_3\text{O}_7^- + \text{CO}_2$) and the resulting $\text{AuTi}_3\text{O}_7^-$ is inert towards CO.^[14a] In sharp contrast, cluster Au_2VO_4^- doped with an Au₂ dimer and having an O_2^{2-} species can oxidize two CO molecules consecutively. The O_2^{2-} species can oxidize CO directly ($\text{I2} \rightarrow \text{I3}'$ in Figure 2a) or indirectly by activation through cleavage into two atomic OS O^{2-} ($\text{I4} \rightarrow \text{I5}$, followed by reaction (6) in Figure 2b). The DFT calculations predicted that the indirect process is more favorable.

The nature of gold bonding in the Au₂ dimer reaction system (Figure 2) is very dynamic. To deliver CO for oxidation by the O^{2-} species on the cluster support, the V–O–Au₂–Au₁ bond in Au_2VO_4^- is changed to V–O–Au₁–Au₂ in Au_2VO_3^- . Upon oxidation of two CO molecules, the polarity of the gold oxidation state switches twice (anionic \rightarrow cationic \rightarrow anionic) and three times (cationic \rightarrow anionic \rightarrow cationic \rightarrow anionic) for the Au₁ and Au₂ atoms, respectively (Figure 3). The Au–Au bond can be strongly polarized ($\text{Au}^{\delta-}\text{--Au}^{\delta+}$) in systems such as Au_2VO_4^- and Au_2VO_3^- clusters. However, in the cases of intermediates I1 and I6, the polarization of the Au–Au bond is relatively small.

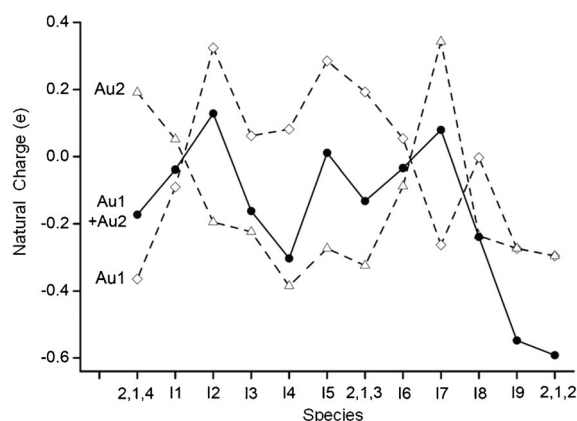


Figure 3. DFT-calculated natural charges on the gold atoms in the reaction intermediates (I1–I9; structures shown in Figure 2) and compounds $\text{Au}_2\text{V}_1\text{O}_4^-$ (denoted 2,1,4), $\text{Au}_2\text{V}_1\text{O}_3^-$ (2,1,3), and $\text{Au}_2\text{V}_1\text{O}_2^-$ (2,1,2).

The dynamic nature of gold bonding^[20] in terms of electron storage and release promotes adsorption and oxidation of CO as well as reduction of the O_2^{2-} species. During the CO adsorption ($2,1,4 \rightarrow \text{I1}$ or $2,1,3 \rightarrow \text{I6}$ in Figure 3), significant negative charge (> 0.1 e) is transferred from the $\text{Au}^{\delta-}$ atom to the neighboring $\text{Au}^{\delta+}$ atom and the VO_x support. The Au₂ dimer in the Au_2VO_4^- reaction system stores a large negative charge (0.44 e) during the first CO oxidation ($\text{I1} \rightarrow \text{I2} \rightarrow \text{I3} \rightarrow \text{I4}$). Additionally, the Au₂–O bond is converted into the Au₂–V bond which is reductive enough to cleave a peroxide O–O bond ($\text{I4} \rightarrow \text{I5}$) and then oxidation of a second CO is possible. In contrast, the Au₁–Ti bond in the previously studied $\text{AuTi}_3\text{O}_8\text{CO}^-$ complex is unable to activate the O_2^{2-} species.^[14a] It can be concluded that incorporation of a gold dimer in the cluster is superior to the incorporation of a gold monomer in the activation of molecular OS.

For comparison with the gas-phase results reported herein, two well-established condensed-phase mechanisms^[3,4] for the oxidation of CO on bulk-oxide-supported gold nanoparticles (NPs) are depicted in Figure 4. Upon consideration of the data, it is clear that the gas-phase and condensed-phase mechanisms parallel each other quite well. The condensed-phase studies have proposed that bulk-oxide-supported Au NPs (where TiO_2 is the bulk oxide) accumulate CO and activate the surface lattice oxygen (O^{2-}) close to the Au NPs in the CO oxidation reaction (Figure 4a). The highly stable O^{2-} species at the perimeter of the Au– TiO_2 interface are removed by reaction with CO through the Au-assisted Mars van Krevelen mechanism and the resulting vacancies can subsequently be replenished by molecular oxygen.^[3] This mechanism parallels that shown in Figure 4c based on the

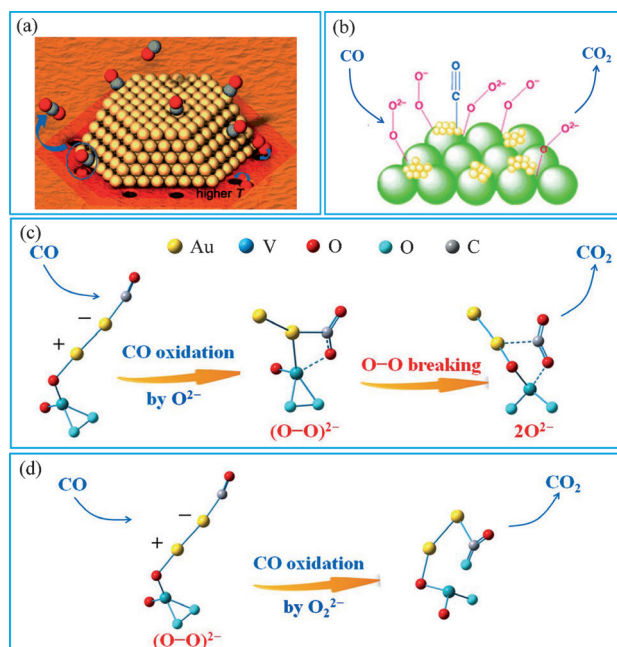


Figure 4. A comparison of the mechanisms of CO oxidation from previous studies of bulk-oxide-supported gold nanoparticles (a, b) and results on oxide-cluster-supported gold dimers (c, d) reported herein. Panels (a) and (b) are adapted from Refs. [3] and [4], respectively. Panels (c) and (d) are derived from Figure 2a.

results obtained herein for the gas-phase study. In this case, the gold dimer captures and then delivers CO for oxidation by the O_2^{2-} species on the cluster support and the molecular OS O_2^{2-} then dissociates to supply additional O^{2-} for further CO oxidation. Moreover, Raman spectroscopy measurements have indicated that the bulk-oxide support (CeO_2) can participate directly in CO oxidation by supplying molecular OS (superoxides and peroxides) at the perimeter of the gold-oxide interface (Figure 4b).^[4] This mechanism then parallels that depicted in Figure 4d: the peroxide species O_2^{2-} can react directly with CO trapped by the gold dimer. This cluster study (Figure 2a) suggests that the direct participation of molecular OS in CO oxidation (Figure 4b,d) can be slightly less favorable than the indirect mechanism (Figure 4a,c). Additionally, this work reveals that the dynamic nature of gold bonding is important for both CO oxidation and O–O reduction.

In conclusion, the consecutive oxidation of two CO molecules by an atomic cluster ($Au_2VO_4^-$) with a closed-shell electronic structure has been demonstrated for the first time. The nature of gold bonding in the Au_2 -doped oxide cluster is very dynamic, which promotes both oxidation of CO and reduction of the peroxide species O_2^{2-} . The oxide cluster containing a gold dimer is found to be superior to that containing a single gold atom in the activation of molecular oxygen species bonded to the ETM center. The mechanism of CO oxidation by the Au_2 -doped oxide cluster $Au_2VO_4^-$ corresponds well to the behavior of related condensed-phase systems. These results provide new insight into the elementary reactions governing the behavior of gold in oxide-supported gold catalysts for catalytic CO oxidation.

Experimental Section

The $Au_2VO_3^-$ and $Au_2VO_4^-$ clusters were generated by laser ablation of an Au/V mixed metal disk (mole ratio Au:V = 1:1) in the presence of 0.5% O_2 in He carrier gas (8 atm). The clusters of interest were selected by mass using a quadrupole mass filter (QMF). To separate $Au_2VO_x^-$ from $AuV_3O_{x+6}^-$ and increase the ion transmittance of the QMF, $^{18}O_2$ was used as the oxygen source to generate the clusters (Figure S1). The mass-selected cluster ions entered into a linear ion-trap reactor where they were thermalized by collisions with a pulse of He gas for about 1.0 ms, followed by interactions with a pulse of $C^{16}O$ for a period of time. A reflectron time-of-flight mass spectrometer was used to detect the cluster ions.^[15] The details of the DFT calculations are given in the Supporting Information.

Acknowledgements

This work is supported by the National Natural Science Foundation of China (Nos. 21325314, 21303215, and 21107026), the Major Research Plan of China (Nos. 2013CB834603 and 2011CB932302), and the Fundamental Research Funds for the Central Universities (No. 2013ZZ0073).

Keywords: atomic clusters · CO oxidation · density functional computations · gold · mass spectrometry

How to cite: *Angew. Chem. Int. Ed.* **2015**, *54*, 11720–11724
Angew. Chem. **2015**, *127*, 11886–11890

- [1] a) M. Haruta, T. Kobayashi, H. Sano, N. Yamada, *Chem. Lett.* **1987**, *16*, 405–408; b) M. Haruta, *Catal. Today* **1997**, *36*, 153–166.
- [2] a) H. Liu, A. I. Kozlov, A. P. Kozlova, T. Shido, K. Asakura, Y. Iwasawa, *J. Catal.* **1999**, *185*, 252–264; b) P. Konova, A. Naydenov, C. Venkov, D. Mehandjiev, D. Andreeva, T. Tabakova, *J. Mol. Catal. A* **2004**, *213*, 235–240; c) P. Konova, A. Naydenov, T. Tabakova, D. Mehandjiev, *Catal. Commun.* **2004**, *5*, 537–542; d) P. Pykkö, *Chem. Soc. Rev.* **2008**, *37*, 1967–1997; e) D. Widmann, Y. Liu, F. Schüth, R. J. Behm, *J. Catal.* **2010**, *276*, 292–305.
- [3] D. Widmann, R. J. Behm, *Angew. Chem. Int. Ed.* **2011**, *50*, 10241–10245; *Angew. Chem.* **2011**, *123*, 10424–10428.
- [4] J. Guzman, S. Carrettin, J. C. Fierro-Gonzalez, Y.-L. Hao, B. C. Gates, A. Corma, *Angew. Chem. Int. Ed.* **2005**, *44*, 4778–4781; *Angew. Chem.* **2005**, *117*, 4856–4859.
- [5] a) R. M. Finch, N. A. Hodge, G. J. Hutchings, A. Meagher, Q. Pankhurst, M. R. H. Siddiqui, F. E. Wagner, R. Whyman, *Phys. Chem. Chem. Phys.* **1999**, *1*, 485–489; b) M. M. Schubert, S. Hackenberg, A. C. van Veen, M. Muhler, V. Plzak, R. J. Behm, *J. Catal.* **2001**, *197*, 113–122; c) J. A. van Bokhoven, C. Louis, J. T. Miller, M. Tromp, O. V. Safonova, P. Glatzel, *Angew. Chem. Int. Ed.* **2006**, *45*, 4651–4654; *Angew. Chem.* **2006**, *118*, 4767–4770; d) M. Kotobuki, R. Leppelt, D. Hansgen, D. Widmann, R. J. Behm, *J. Catal.* **2009**, *264*, 67–76; e) J. Gong, C. B. Mullins, *Acc. Chem. Res.* **2009**, *42*, 1063–1073; f) T. Fujitani, I. Nakamura, *Angew. Chem. Int. Ed.* **2011**, *50*, 10144–10147; *Angew. Chem.* **2011**, *123*, 10326–10329.
- [6] a) M. Valden, X. Lai, D. W. Goodman, *Science* **1998**, *281*, 1647–1650; b) R. J. Davis, *Science* **2003**, *301*, 926–927; c) C. T. Campbell, *Science* **2004**, *306*, 234–235.
- [7] a) C. K. Costello, M. C. Kung, H.-S. Oh, Y. Wang, H. H. Kung, *Appl. Catal. A* **2002**, *232*, 159–168; b) Z.-P. Liu, X.-Q. Gong, J. Kohanoff, C. Sanchez, P. Hu, *Phys. Rev. Lett.* **2003**, *91*, 266102; c) I. N. Remediakis, N. Lopez, J. K. Nørskov, *Angew. Chem. Int. Ed.* **2005**, *44*, 1824–1826; *Angew. Chem.* **2005**, *117*, 1858–1860; d) J.-D. Grunwaldt, A. Baiker, *J. Phys. Chem. B* **1999**, *103*, 1002–1012; e) S. Carrettin, Y. Hao, V. Aguilar-Guerrero, B. C. Gates, S. Trasobares, J. J. Calvino, A. Corma, *Chem. Eur. J.* **2007**, *13*, 7771–7779; f) M. Boronat, A. Corma, *Dalton Trans.* **2010**, *39*, 8538–8546; g) J. D. Stiehl, T. S. Kim, S. M. McClure, C. B. Mullins, *J. Am. Chem. Soc.* **2004**, *126*, 13574–13575.
- [8] a) M. Che, A. J. Tench, *Adv. Catal.* **1982**, *31*, 77–133; b) G. I. Panov, K. A. Dubkov, E. V. Starokon, *Catal. Today* **2006**, *117*, 148–155.
- [9] D. Widmann, R. J. Behm, *Acc. Chem. Res.* **2014**, *47*, 740–749.
- [10] S. Carrettin, P. Concepción, A. Corma, J. M. L. Nieto, V. F. Puentes, *Angew. Chem. Int. Ed.* **2004**, *43*, 2538–2540; *Angew. Chem.* **2004**, *116*, 2592–2594.
- [11] a) R. A. J. O'Hair, G. N. Khairallah, *J. Cluster Sci.* **2004**, *15*, 331–363; b) D. K. Böhme, H. Schwarz, *Angew. Chem. Int. Ed.* **2005**, *44*, 2336–2354; *Angew. Chem.* **2005**, *117*, 2388–2406; c) T. M. Bernhardt, *Int. J. Mass Spectrom.* **2005**, *243*, 1–9; d) A. W. Castleman, Jr., *Catal. Lett.* **2011**, *141*, 1243–1253; e) S. Yin, E. R. Bernstein, *Int. J. Mass Spectrom.* **2012**, *321/322*, 49–65; f) S. M. Lang, T. M. Bernhardt, *Phys. Chem. Chem. Phys.* **2012**, *14*, 9255–9269; g) M. Schlangen, H. Schwarz, *Catal. Lett.* **2012**, *142*, 1265–1278; h) Q.-Y. Liu, S.-G. He, *Chem. J. Chin. Univ.* **2014**, *35*, 665–688.
- [12] a) H. Häkkinen, U. Landman, *J. Am. Chem. Soc.* **2001**, *123*, 9704–9705; b) W. T. Wallace, R. L. Whetten, *J. Am. Chem. Soc.* **2002**, *124*, 7499–7505; c) L. D. Socaciu, J. Hagen, T. M. Bernhardt, L. Wöste, U. Heiz, H. Häkkinen, U. Landman, *J. Am. Chem. Soc.* **2003**, *125*, 10437–10445; d) M. L. Kimble, A. W.

- Castleman, Jr., R. Mitrić, C. Bürgel, V. Bonačić-Koutecký, *J. Am. Chem. Soc.* **2004**, *126*, 2526–2535; e) M. L. Kimble, N. A. Moore, A. W. Castleman, Jr., C. Bürgel, R. Mitrić, V. Bonačić-Koutecký, *Eur. Phys. J. D* **2007**, *43*, 205–208; f) C. Bürgel, N. M. Reilly, G. E. Johnson, R. Mitrić, M. L. Kimble, A. W. Castleman, Jr., V. Bonačić-Koutecký, *J. Am. Chem. Soc.* **2008**, *130*, 1694–1698.
- [13] a) G. E. Johnson, R. Mitrić, E. C. Tyo, V. Bonačić-Koutecký, A. W. Castleman, Jr., *J. Am. Chem. Soc.* **2008**, *130*, 13912–13920; b) Z. Yuan, Y. X. Zhao, X. N. Li, S. G. He, *Int. J. Mass Spectrom.* **2013**, *354/355*, 105–112; c) Z.-C. Wang, S. Yin, E. R. Bernstein, *Phys. Chem. Chem. Phys.* **2013**, *15*, 10429–10434; d) X.-N. Wu, J.-B. Ma, B. Xu, Y.-X. Zhao, X.-L. Ding, S.-G. He, *J. Phys. Chem. A* **2011**, *115*, 5238–5246; e) J.-B. Ma, B. Xu, J.-H. Meng, X.-N. Wu, X.-L. Ding, X.-N. Li, S.-G. He, *J. Am. Chem. Soc.* **2013**, *135*, 2991–2998.
- [14] a) X.-N. Li, Z. Yuan, S.-G. He, *J. Am. Chem. Soc.* **2014**, *136*, 3617–3623; b) Z. Yuan, X.-N. Li, S.-G. He, *J. Phys. Chem. Lett.* **2014**, *5*, 1585–1590; c) Z.-Y. Li, Z. Yuan, X.-N. Li, Y.-X. Zhao, S.-G. He, *J. Am. Chem. Soc.* **2014**, *136*, 14307–14313; d) H. Himeno, K. Miyajima, T. Yasuike, F. Mafuné, *J. Phys. Chem. A* **2011**, *115*, 11479–11485.
- [15] Z. Yuan, Z.-Y. Li, Z.-X. Zhou, Q.-Y. Liu, Y.-X. Zhao, S.-G. He, *J. Phys. Chem. C* **2014**, *118*, 14967–14976.
- [16] a) G. Kummerlöwe, M. K. Beyer, *Int. J. Mass Spectrom.* **2005**, *244*, 84–90; b) T. Su, M. T. Bowers, *J. Chem. Phys.* **1973**, *58*, 3027–3037.
- [17] a) G. E. Johnson, R. Mitrić, M. Nössler, E. C. Tyo, V. Bonačić-Koutecký, A. W. Castleman, Jr., *J. Am. Chem. Soc.* **2009**, *131*, 5460–5470; b) X. N. Wu, X. L. Ding, S. M. Bai, B. Xu, S. G. He, Q. Shi, *J. Phys. Chem. C* **2011**, *115*, 13329–13337.
- [18] J.-B. Ma, Z.-C. Wang, M. Schlangen, S.-G. He, H. Schwarz, *Angew. Chem. Int. Ed.* **2013**, *52*, 1226–1230; *Angew. Chem.* **2013**, *125*, 1264–1268.
- [19] Z.-C. Wang, N. Dietl, R. Kretschmer, T. Weiske, M. Schlangen, H. Schwarz, *Angew. Chem. Int. Ed.* **2011**, *50*, 12351–12354; *Angew. Chem.* **2011**, *123*, 12559–12562.
- [20] a) H. Schwarz, *Angew. Chem. Int. Ed.* **2003**, *42*, 4442–4454; *Angew. Chem.* **2003**, *115*, 4580–4593; b) P. Pyykkö, *Angew. Chem. Int. Ed.* **2004**, *43*, 4412–4456; *Angew. Chem.* **2004**, *116*, 4512–4557; c) L. S. Wang, *Phys. Chem. Chem. Phys.* **2010**, *12*, 8694–8705; d) Y.-G. Wang, D. Mei, V. Glezakou, J. Li, R. Rousseau, *Nat. Commun.* **2015**, *6*, 6511.

Received: June 15, 2015

Revised: July 14, 2015

Published online: August 12, 2015